

## Supporting Information

# Novel Phosphorus (V) Tetrabenzotriazacorroles: Synthesis, Characterization, Optical, Electrochemical, and Femtosecond Nonlinear Optical Studies

K. S. Srivishnu,<sup>a,b</sup> Manne Naga Rajesh,<sup>a,b</sup> Dipanjan Banerjee,<sup>c</sup>  
Venugopal Rao Soma,<sup>c,\*</sup> Lingamallu Giribabu<sup>a,b,\*</sup>

<sup>a</sup>Polymers & Functional Materials Division, Tarnaka, CSIR-Indian Institute of Chemical Technology, Hyderabad 500007, Telangana, India

<sup>b</sup>Academy of Scientific and Innovative Research (AcSIR), Ghaziabad 201002, India

<sup>c</sup>Advanced Research Centre for High Energy Materials (ACRHEM), University of Hyderabad, Hyderabad 500046, Telangana, India

Corresponding Authors' e-mail addresses: [soma\\_venu@uohyd.ac.in](mailto:soma_venu@uohyd.ac.in) (V.R. Soma), [giribabu@iict.res.in](mailto:giribabu@iict.res.in) (L. Giribabu),

Table of Contents		Page No.
Figure S1	<sup>1</sup> H NMR spectrum of 1 in CDCl <sub>3</sub> .	S4
Figure S2	ESI-MS spectrum of 1.	S4
Figure S3	<sup>1</sup> H NMR spectrum of 2 in CDCl <sub>3</sub> .	S5
Figure S4	ESI-MS spectrum of 2.	S5
Figure S5	<sup>1</sup> H NMR spectrum of <b>TBC-tert</b> in CDCl <sub>3</sub> .	S6
Figure S6	<sup>31</sup> P NMR of <b>TBC-tert</b> in CDCl <sub>3</sub> .	S6
Figure S7	IR spectrum of <b>TBC-tert</b> .	S7

Figure S8	MALDI-MS spectrum of <b>TBC-<i>tert</i></b> .	S7
Figure S9	<sup>1</sup> H NMR spectrum of <b>TBC-PTZ</b> in CDCl <sub>3</sub> .	S8
Figure S10	<sup>31</sup> P NMR of <b>TBC-PTZ</b> in CDCl <sub>3</sub> .	S8
Figure S11	IR spectrum of <b>TBC-PTZ</b>	S9
Figure S12	MALDI-MS spectrum of <b>TBC-PTZ</b> .	S9
Figure S13	<sup>1</sup> H NMR spectrum of <b>TBC-CBZ</b> in CDCl <sub>3</sub> .	S10
Figure S14	<sup>31</sup> P NMR of <b>TBC-CBZ</b> in CDCl <sub>3</sub> .	S10
Figure S15	IR spectrum of <b>TBC-CBZ</b> .	S11
Figure S16	MALDI-MS spectrum of <b>TBC-CBZ</b> .	S11
Figure S17	Absorption spectra of <b>TBC-CBZ</b> in different solvents.	S12
Figure S18	Absorption spectra of <b>TBC-PTZ</b> in different solvents.	S12
Figure S19	Absorption spectra of <b>TBC-<i>tert</i></b> in DCM at various concentrations.	S13
Figure S20	Absorption spectra of <b>TBC-PTZ</b> in DCM at various concentrations.	S13
Figure S21	Fluorescence spectra of <b>TBC-<i>tert</i></b> in various solvents.	S14
Figure S22	Fluorescence spectra of <b>TBC-CBZ</b> in various solvents.	S14
Figure S23	<i>In-situ</i> UV-Vis spectro-electrochemical changes of <b>TBC-CBZ</b> . a) E <sub>app</sub> = 0.90 V b) E <sub>app</sub> = 1.60 V c) E <sub>app</sub> = -1.30 V.	S15
Figure S24	NLO optical data (a) OA (b) CA of DCM solvent under the excitation of femtosecond 1kHz, 50 fs, 800 nm pulses. NLO optical data (c) OA, (d) CA, of DCM solvent under the excitation of femtosecond 80 MHz, 150 fs, 800 nm pulses. 3D blue spheres and red continuous line correspondingly represent experimental data and theoretically fitted curve.	S16

## Methods and instrumentation

<sup>1</sup>H-NMR spectra were recorded using either a 400 or 500 MHz INOVA spectrometer. A Thermo Nicolet Nexus 670 spectrometer was used to record the FTIR spectra using the KBr pellet technique. A Shimadzu Biotech Axima Performance 2.9.3.20110624: Mode Linear, Power spectrometer was used to record Matrix-assisted laser desorption ionization time-of-flight (MALDI-TOF) mass spectra. Cyclic voltammetric measurements were performed using a CHI instruments model CHI 620C potentiostat, as detailed in our previous reports [1]. The spectroelectrochemical studies were also carried out using the same instrument at 25 °C. Pt gauze was the working electrode and Pt wire was the counter electrode. UV-visible spectra were recorded with a Shimadzu spectrophotometer (Model UV-3600). The concentrations of the samples used for these measurements using 1 × 10<sup>-5</sup> M. Steady-state fluorescence spectra were measured using a Fluorolog-3 spectrofluorometer (FluoroLog3 model, JobinYvon), as detailed in our previous reports. Fluorescence lifetime measurements were carried out using a picosecond time-correlated single-photon counting (TCSPC) setup (FluoroLog3-Triple Illuminator, IBH Horiba JobinYvon), employing a picosecond light-emitting diode laser (NanoLED, λ<sub>ex</sub> = 405 nm) as the excitation source.

Ground state geometry optimization of the structures of the TBCs in the gas phase was carried out with DFT studies and the B3LYP method using the 6-31G(d,p) basis set by the Gaussian 09 software on a personal computer [2-4]. TD-DFT (time-dependent density functional theory) was employed for the estimation of ground state to excited state transitions using B3LYP and the 6-31G(d,p) basis set. The geometries were used to obtain the frontier molecular orbitals (FMOs) and were also subjected to single-point TDDFT studies to obtain the UV-Visible spectra of the sensitizers. The integral equation formalism polarizable continuum model (PCM) within the self-consistent reaction field (SCRF) theory was used in the TDDFT calculations to describe the solvation of the dyes in tetrahydrofuran [5,6]. The software GaussSum 2.2.5 was employed to simulate the major portions of the absorption spectra and to interpret the nature of transitions [7,8].

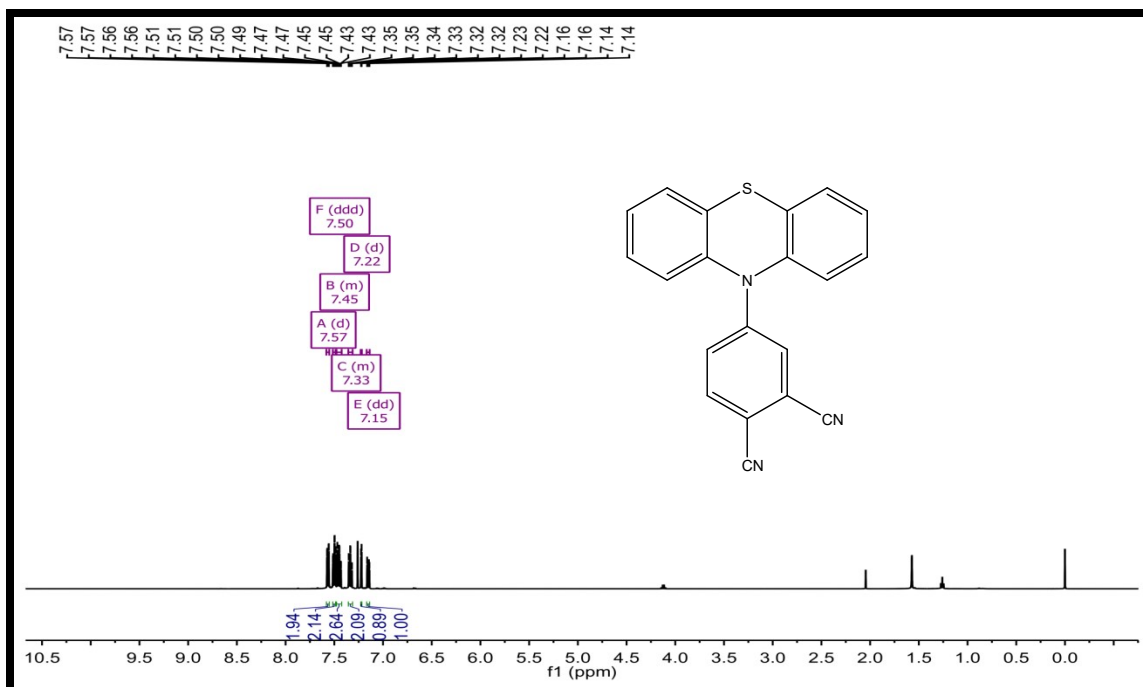


Fig. S1.  $^1\text{H}$  NMR spectrum of 1 in  $\text{CDCl}_3$ .

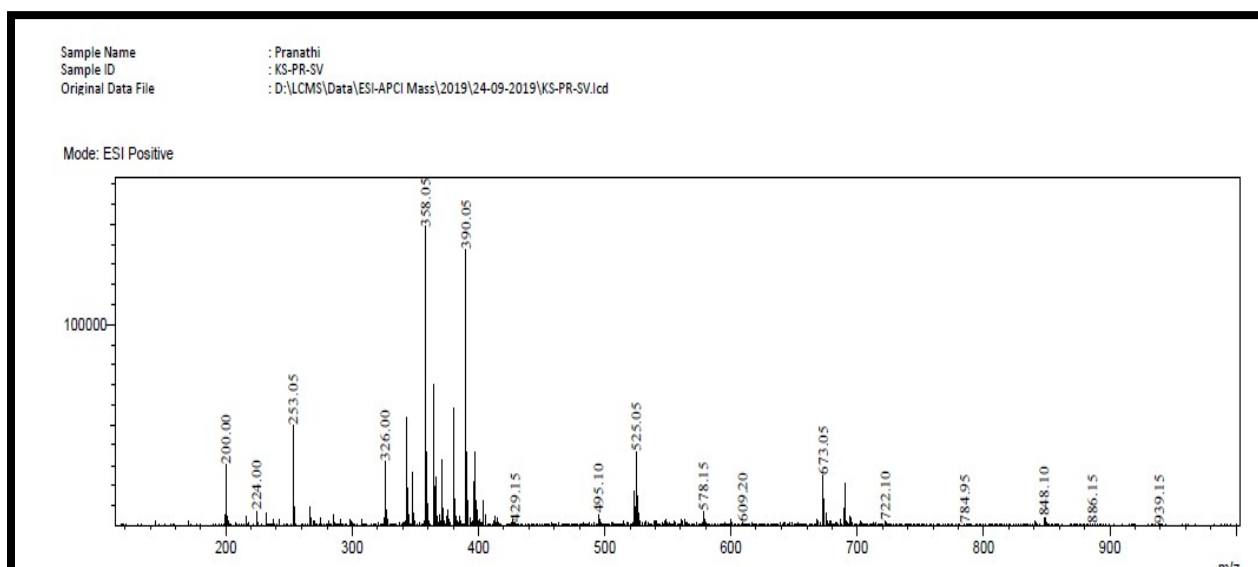


Fig. S2. ESI-MS spectrum of 1.

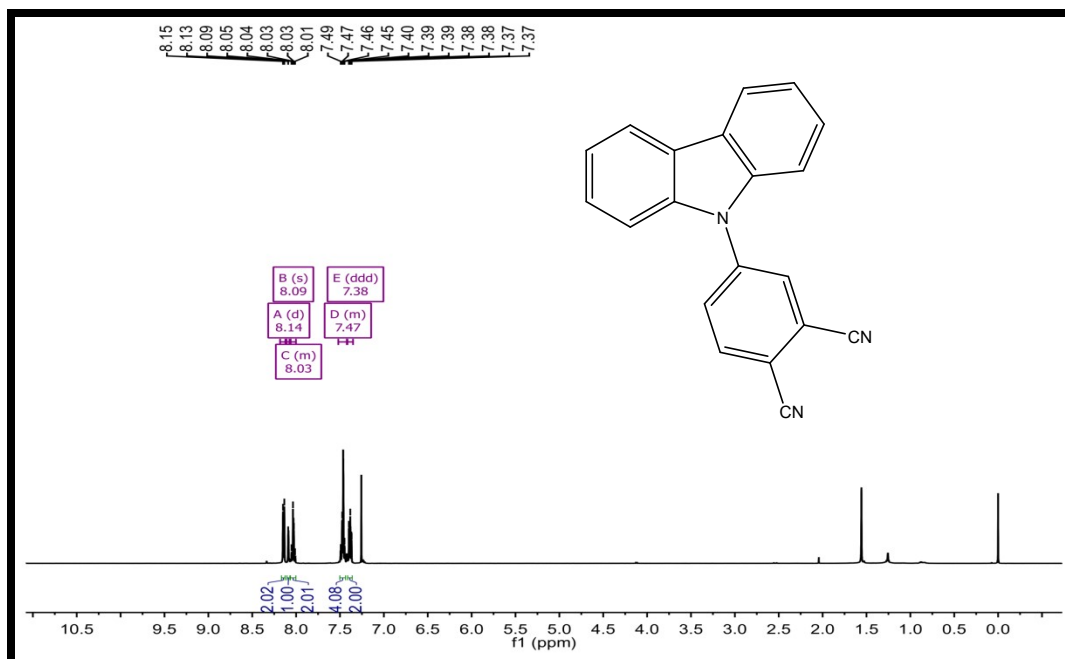


Fig. S3. <sup>1</sup>H NMR spectrum of 2 in CDCl<sub>3</sub>.

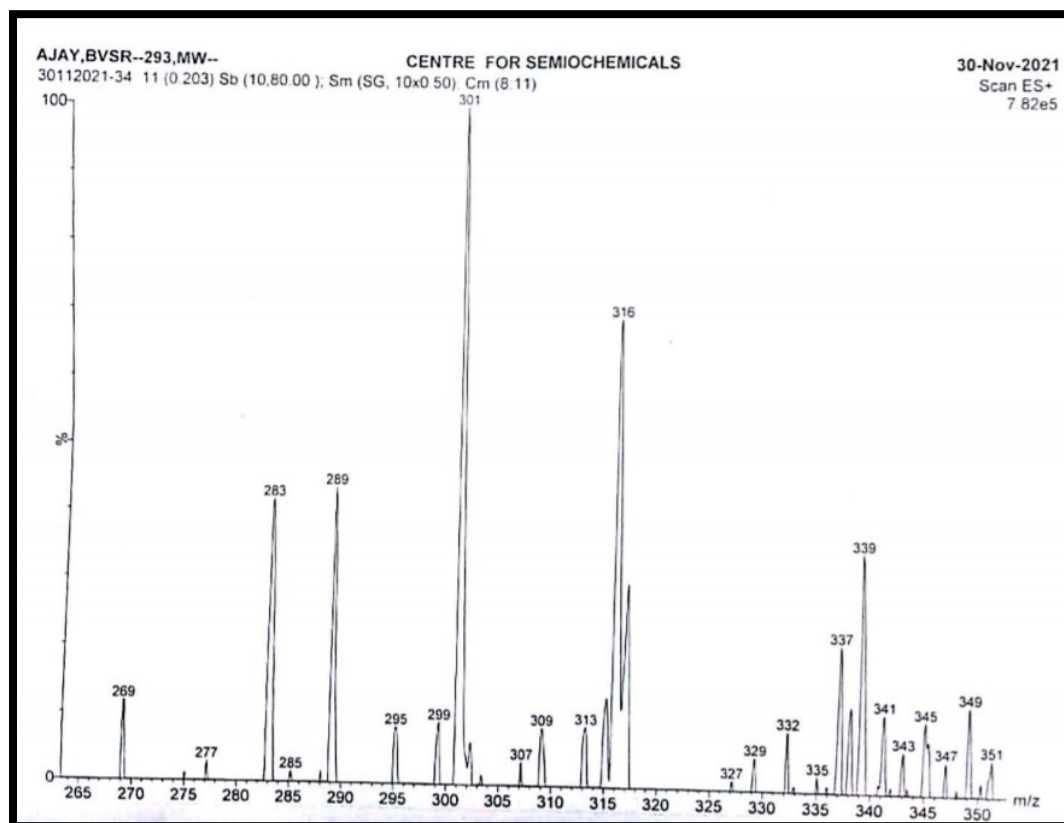


Fig. S4. ESI-MS spectrum of 2.

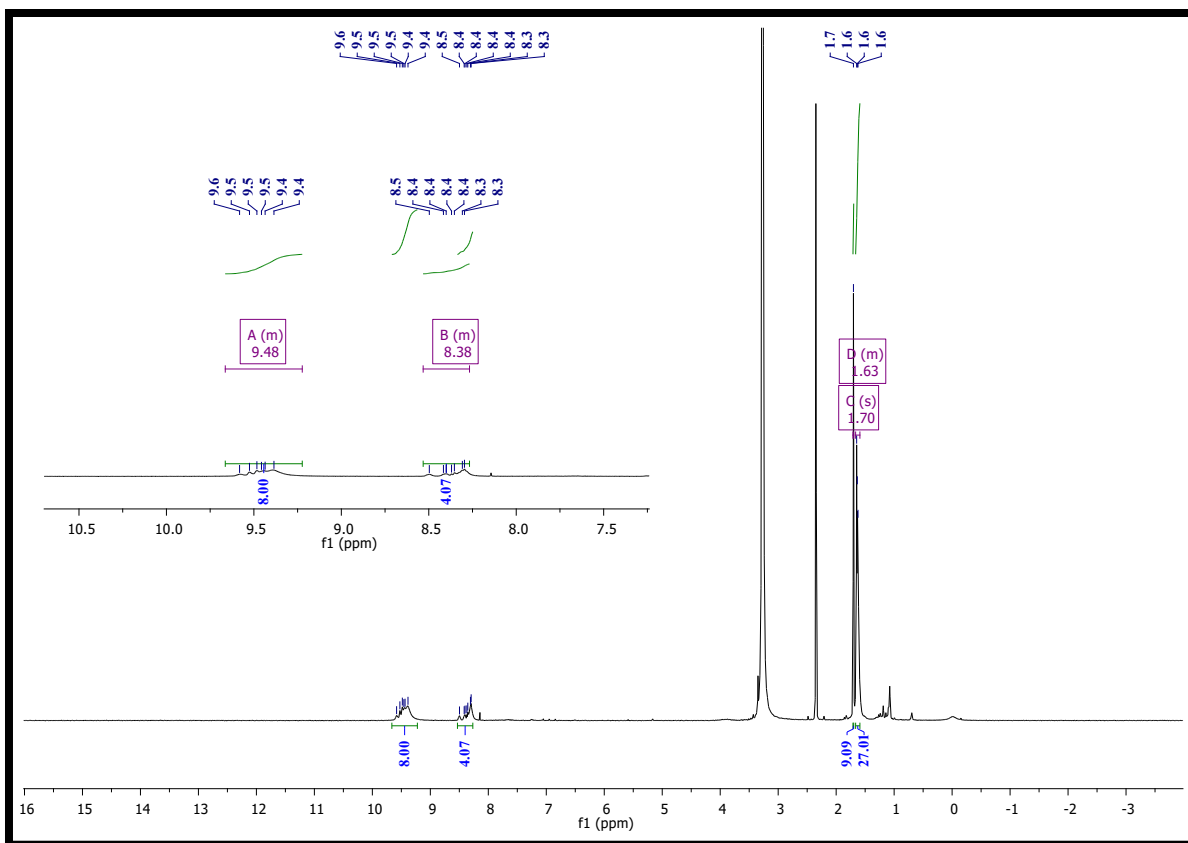


Fig. S5.  $^1\text{H}$  NMR spectrum of TBC-*tert* in DMSO- $d_6$ .

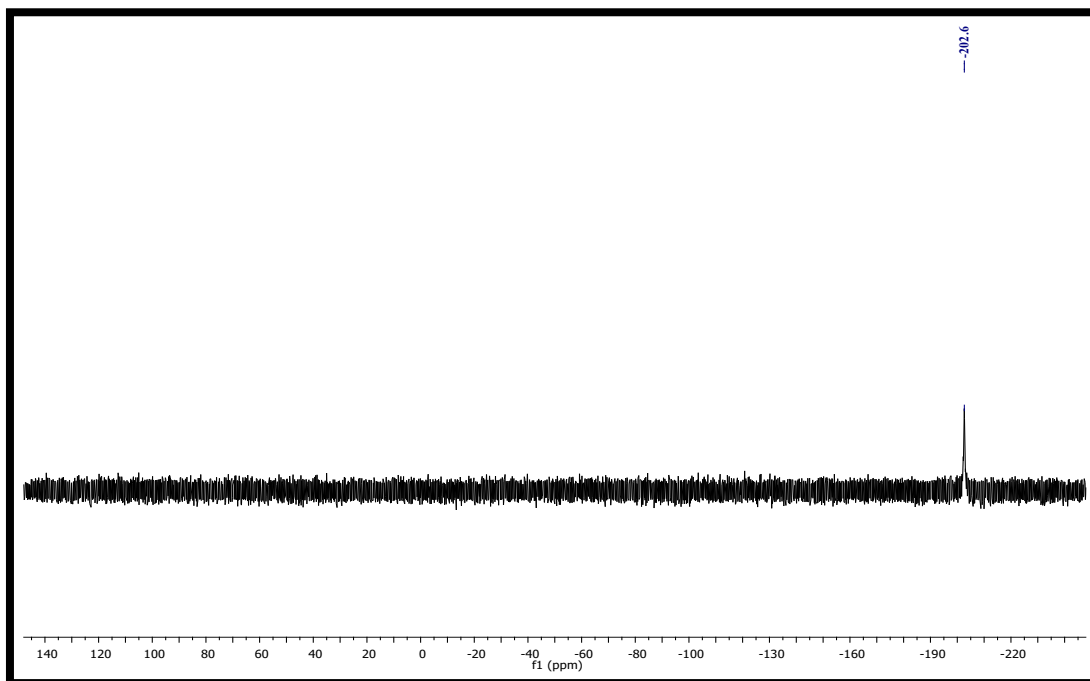


Fig. S6.  $^{31}\text{P}$  NMR of TBC-*tert* in DMSO- $d_6$ .

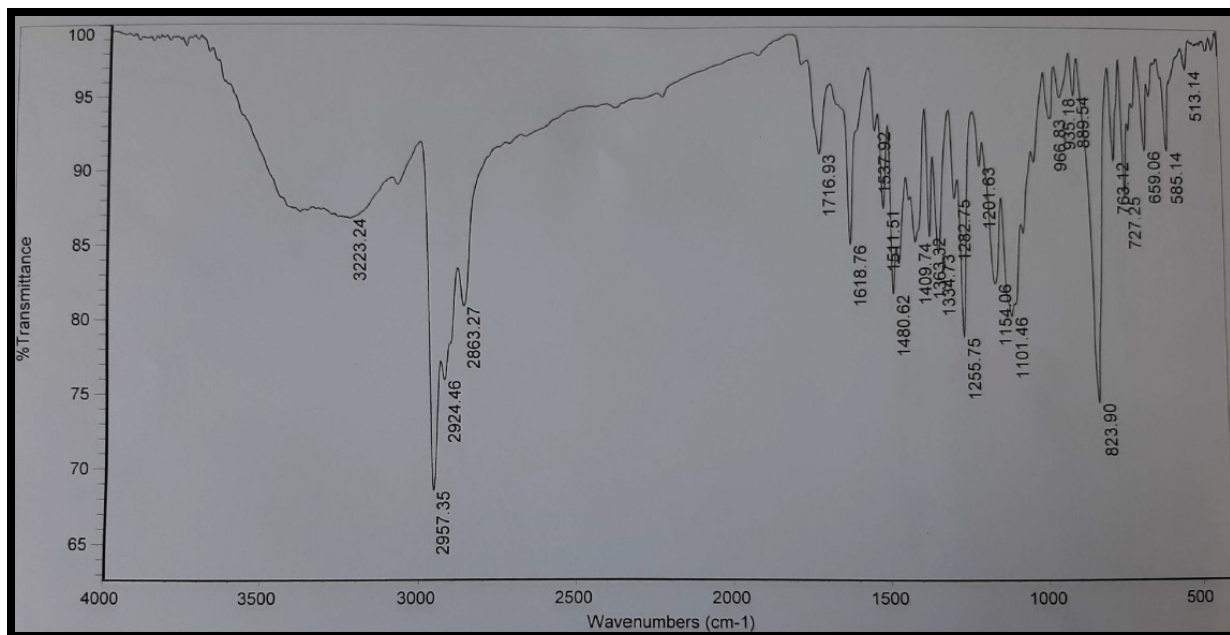


Fig. S7. IR spectrum of TBC-tert.

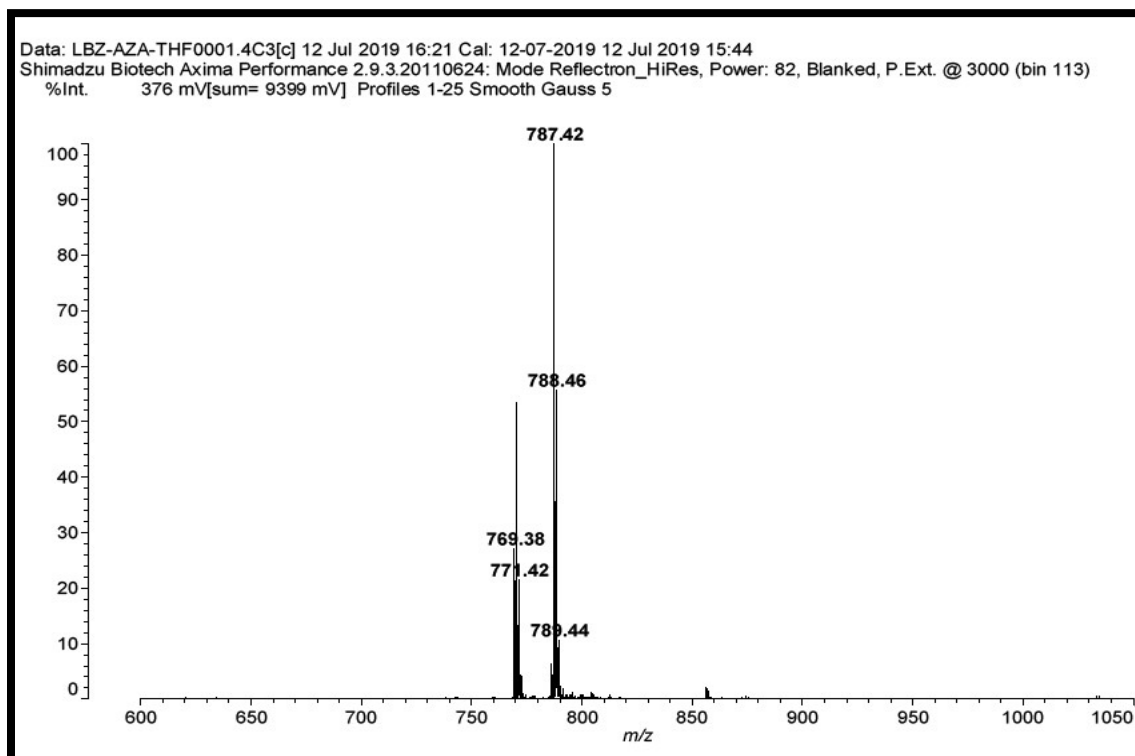


Fig. S8. MALDI-MS spectrum of TBC-tert.

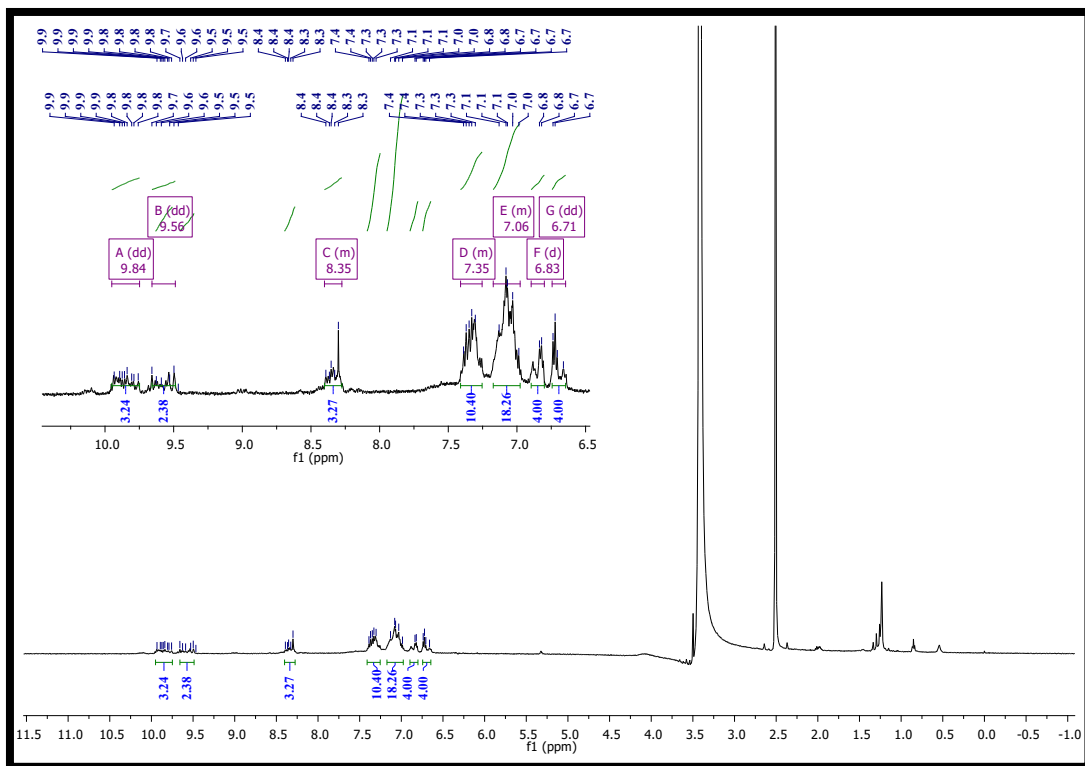


Fig. S9.  $^1\text{H}$  NMR spectrum of TBC-PTZ in  $\text{DMSO-d}_6$ .

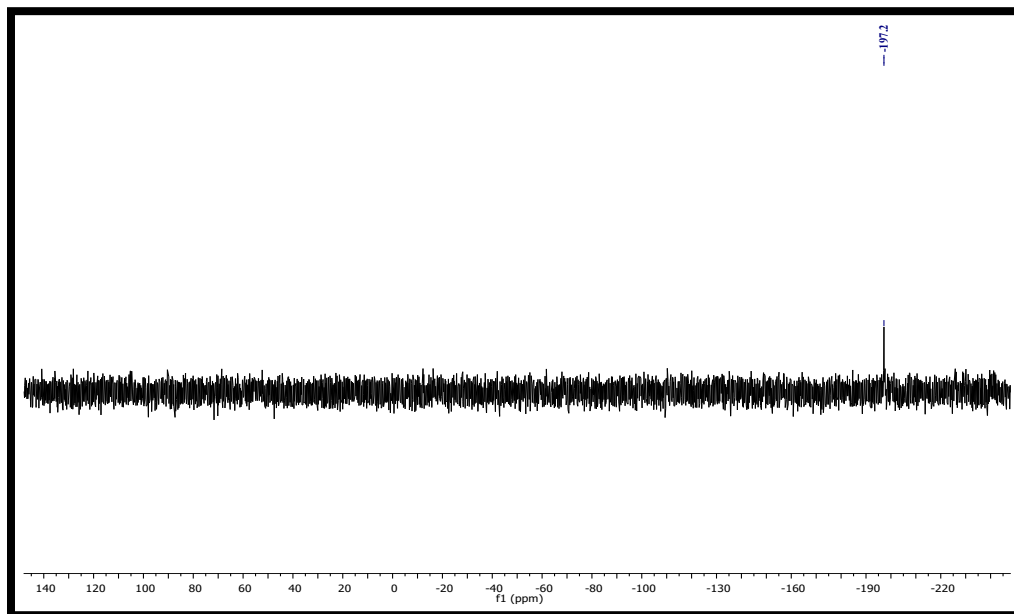


Fig. S10.  $^{31}\text{P}$  NMR of TBC-PTZ in  $\text{CDCl}_3$ .



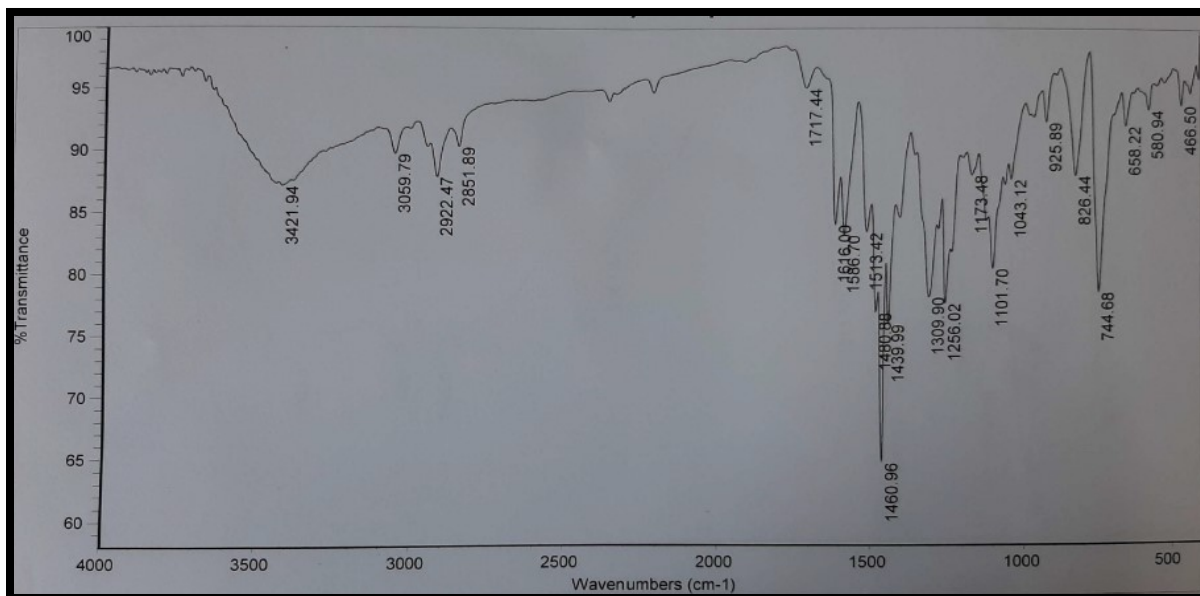


Fig. S11. IR spectrum of TBC-PTZ.

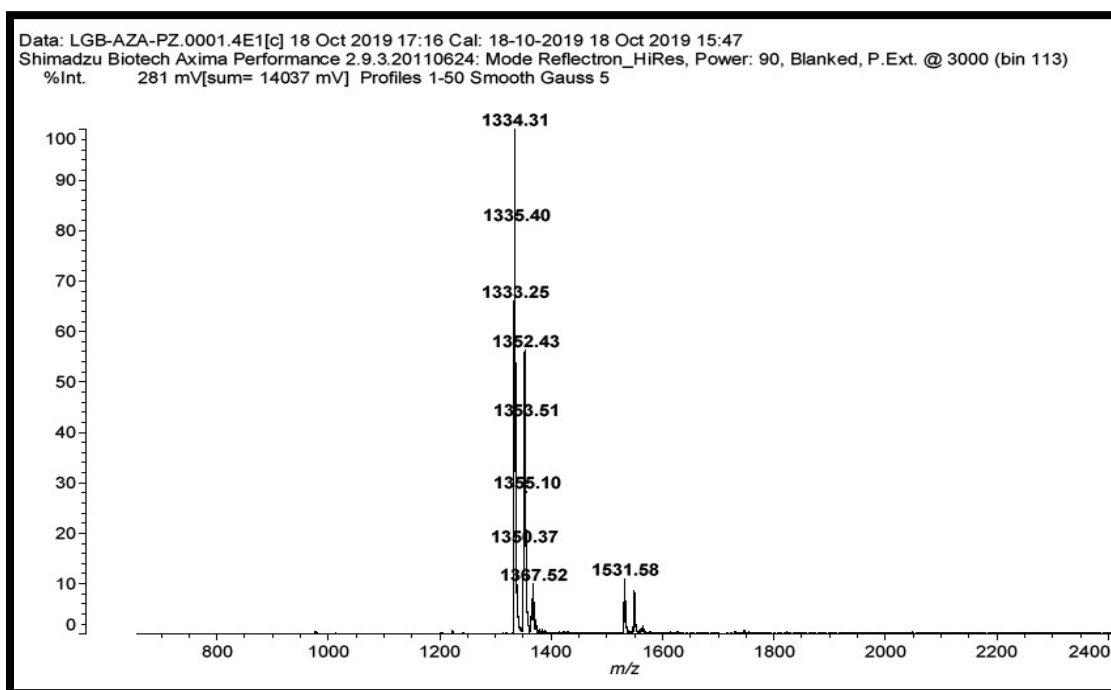


Fig. S12. MALDI-MS spectrum of TBC-PTZ.

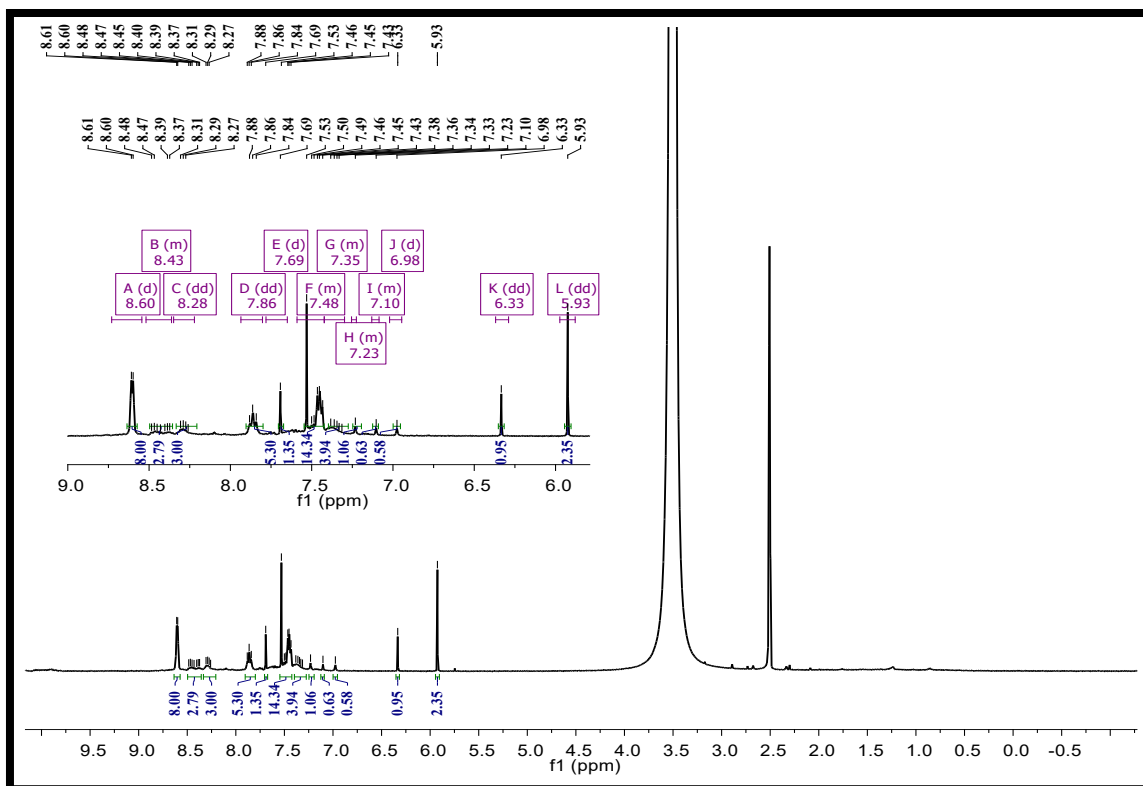


Fig. S13.  $^1\text{H}$  NMR spectrum of TBC-CBZ in  $\text{DMSO-d}_6$ .

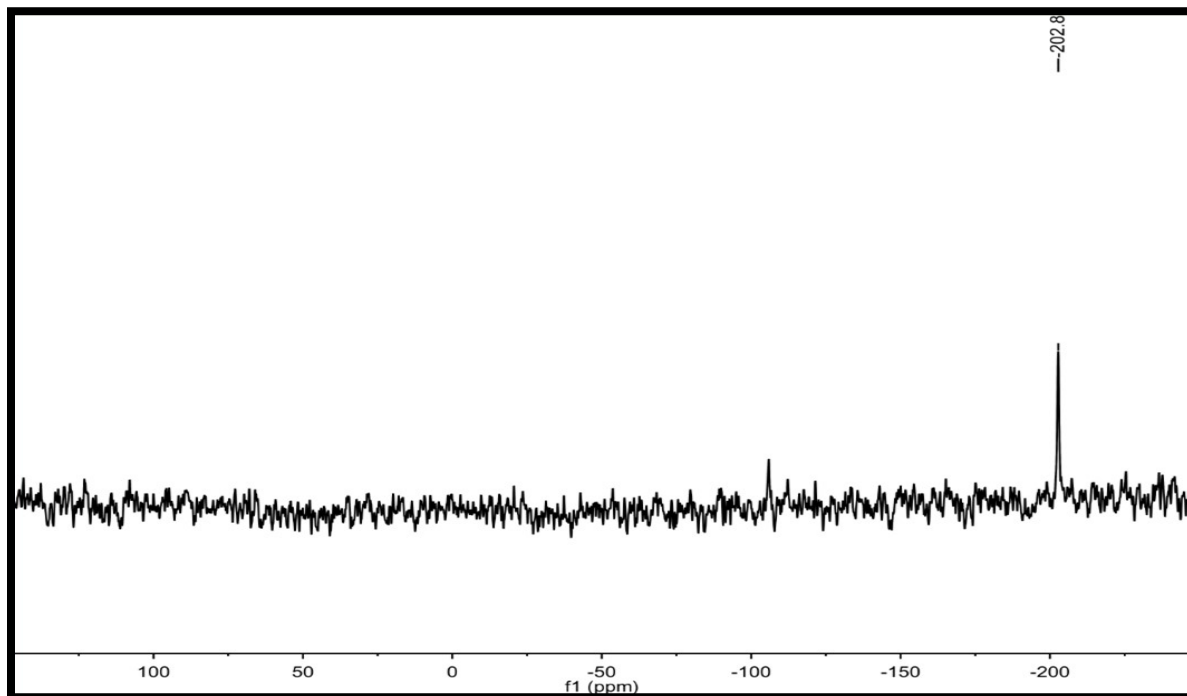


Fig. S14.  $^{31}\text{P}$  NMR of TBC-CBZ in  $\text{DMSO-d}_6$ .

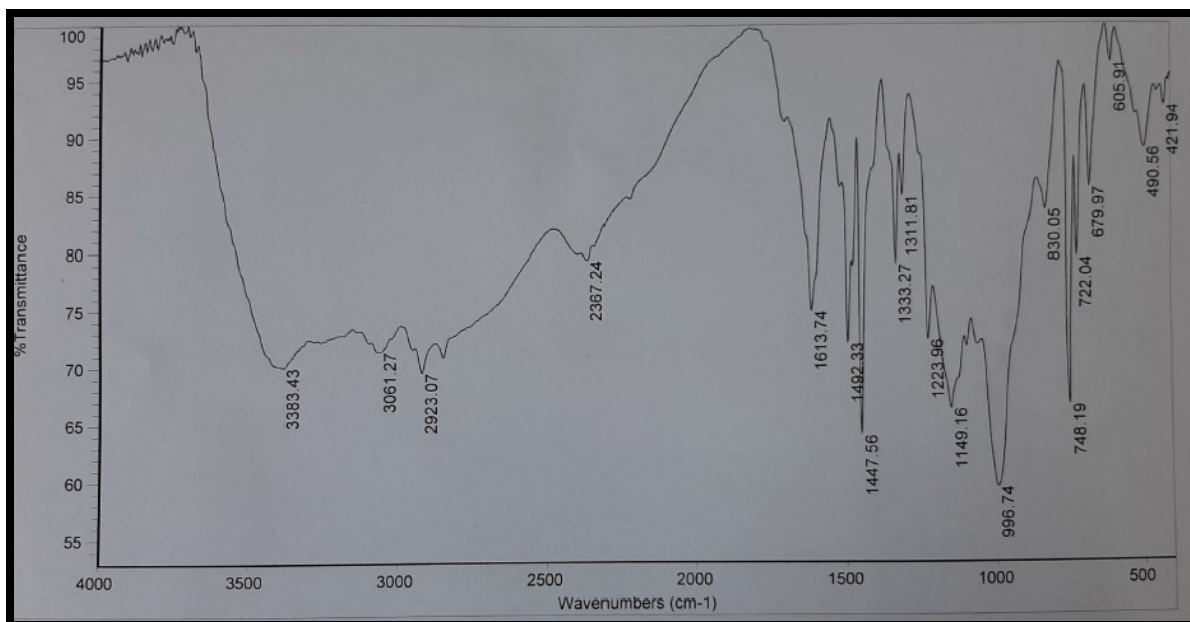


Fig. S15. IR spectrum of TBC-CBZ.

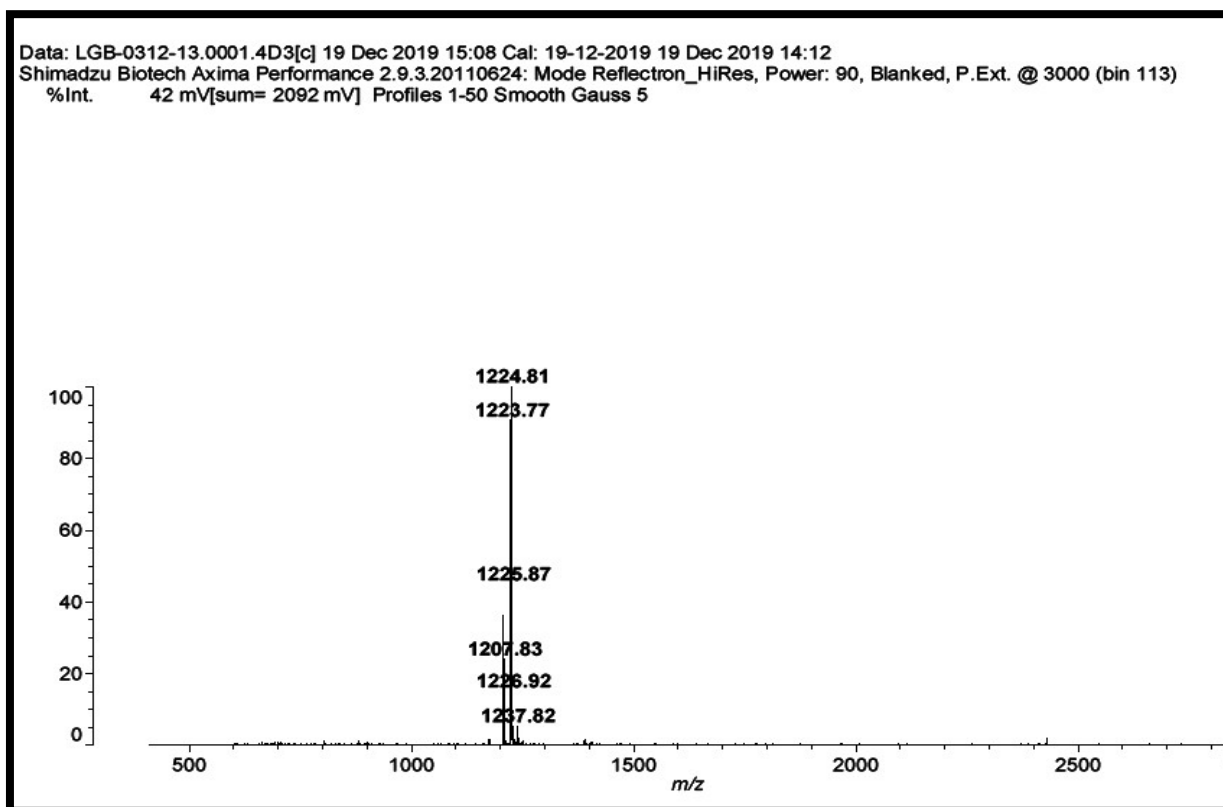


Fig. S16. MALDI-MS spectrum of TBC-CBZ.

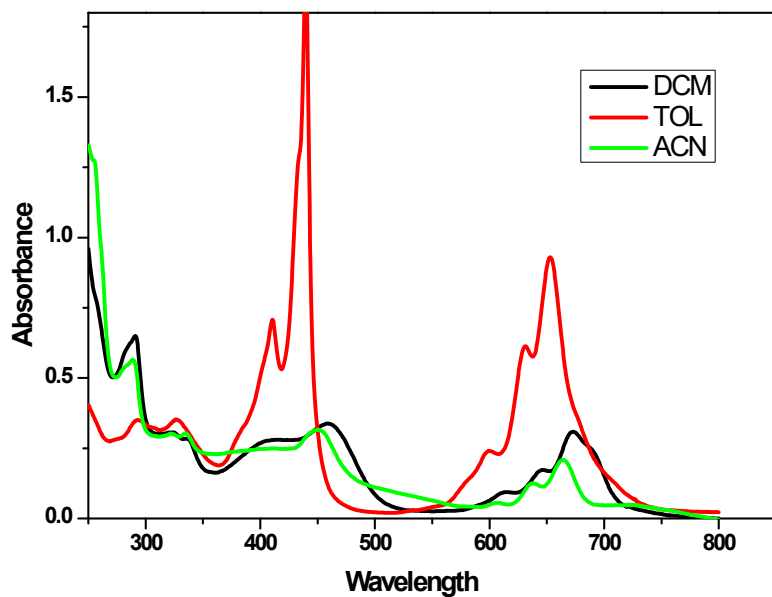


Fig. S17. Absorption spectra of TBC-CBZ in different solvents.

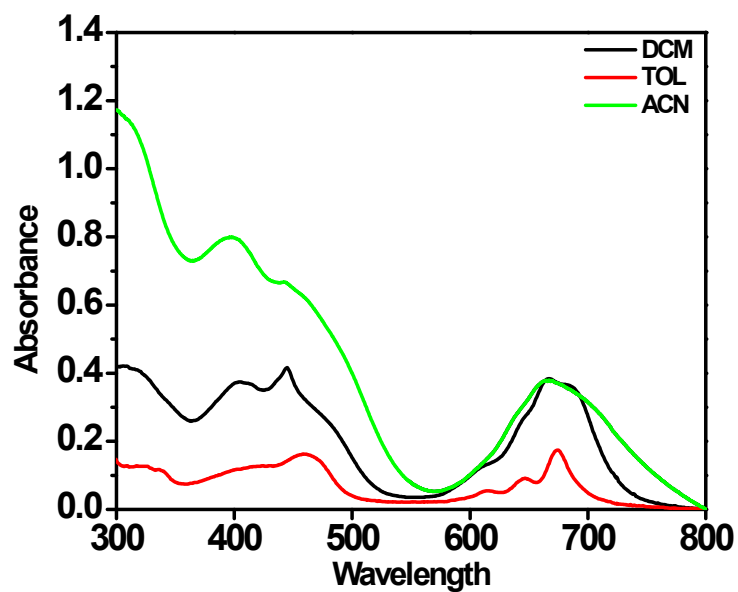


Fig. S18. Absorption spectra of TBC-PTZ in different solvents.

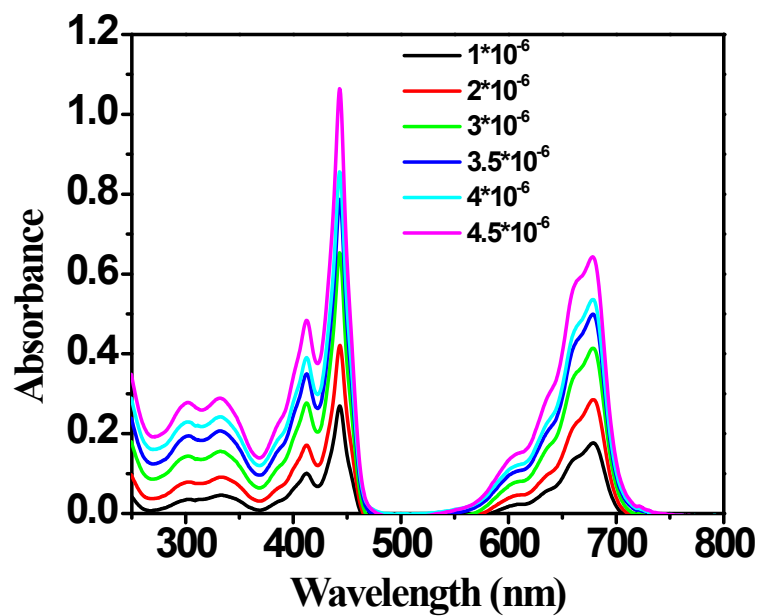


Fig. S19. Absorption spectra of TBC-*tert* in DCM at various concentrations.

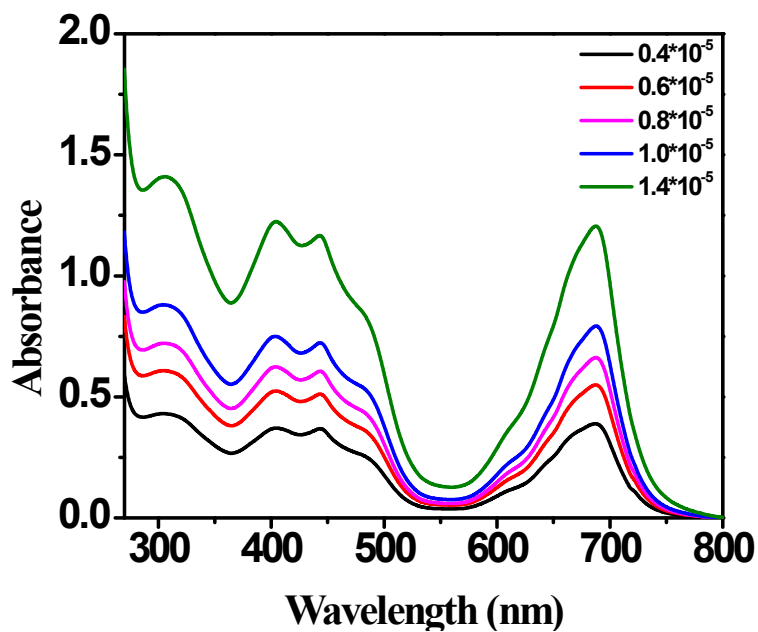


Fig. S20. Absorption spectra of TBC-PTZ in DCM at various concentrations.

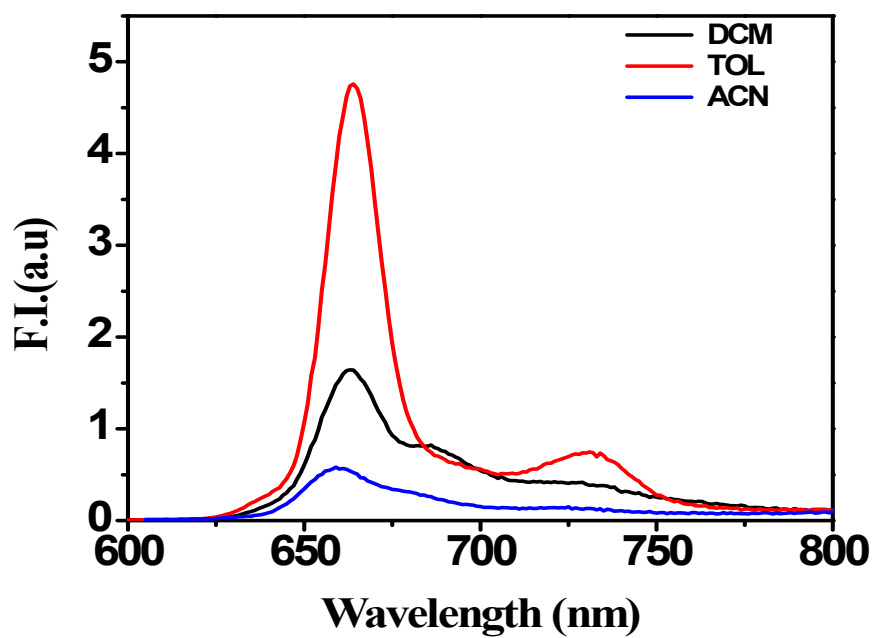


Fig. S21. Fluorescence spectra of TBC-*tert* in various solvents.

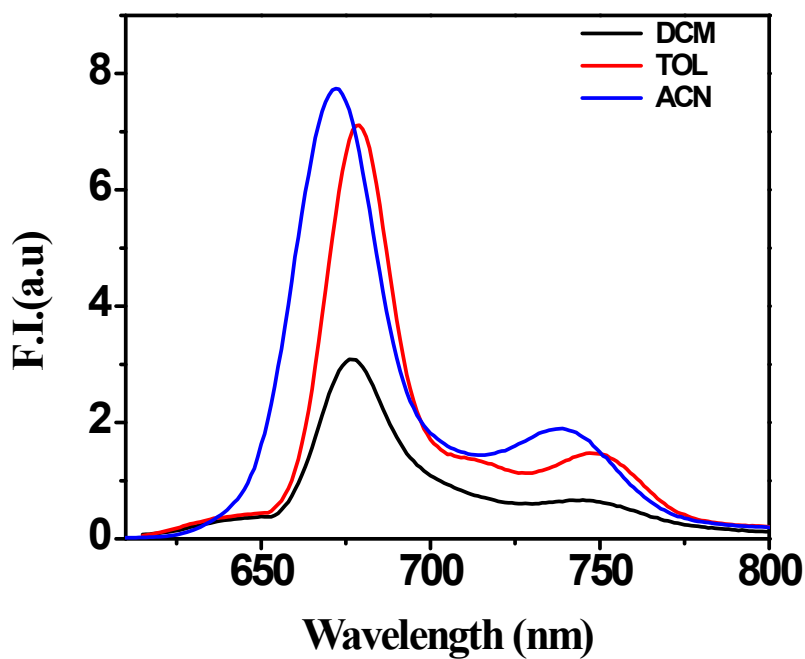
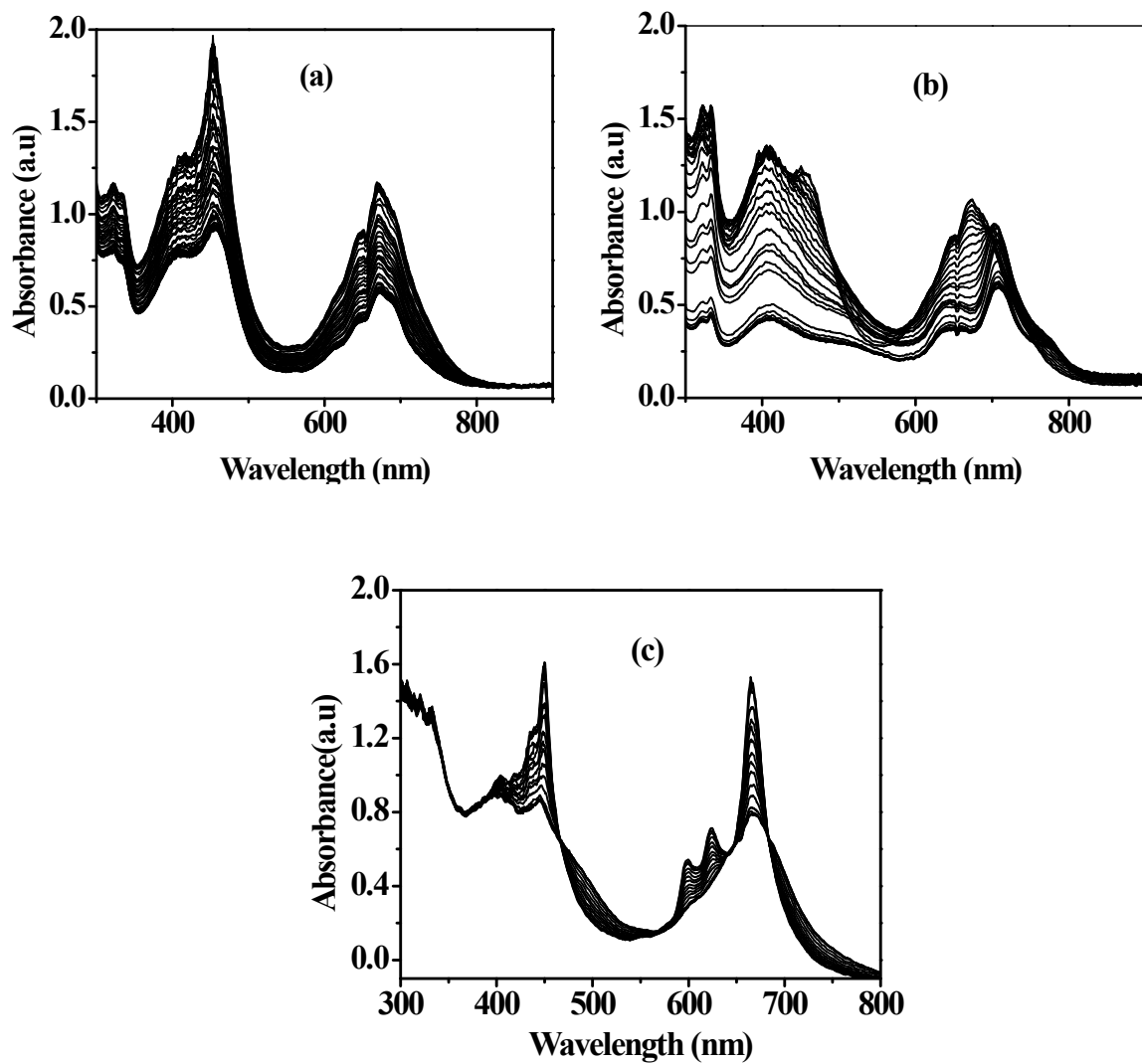
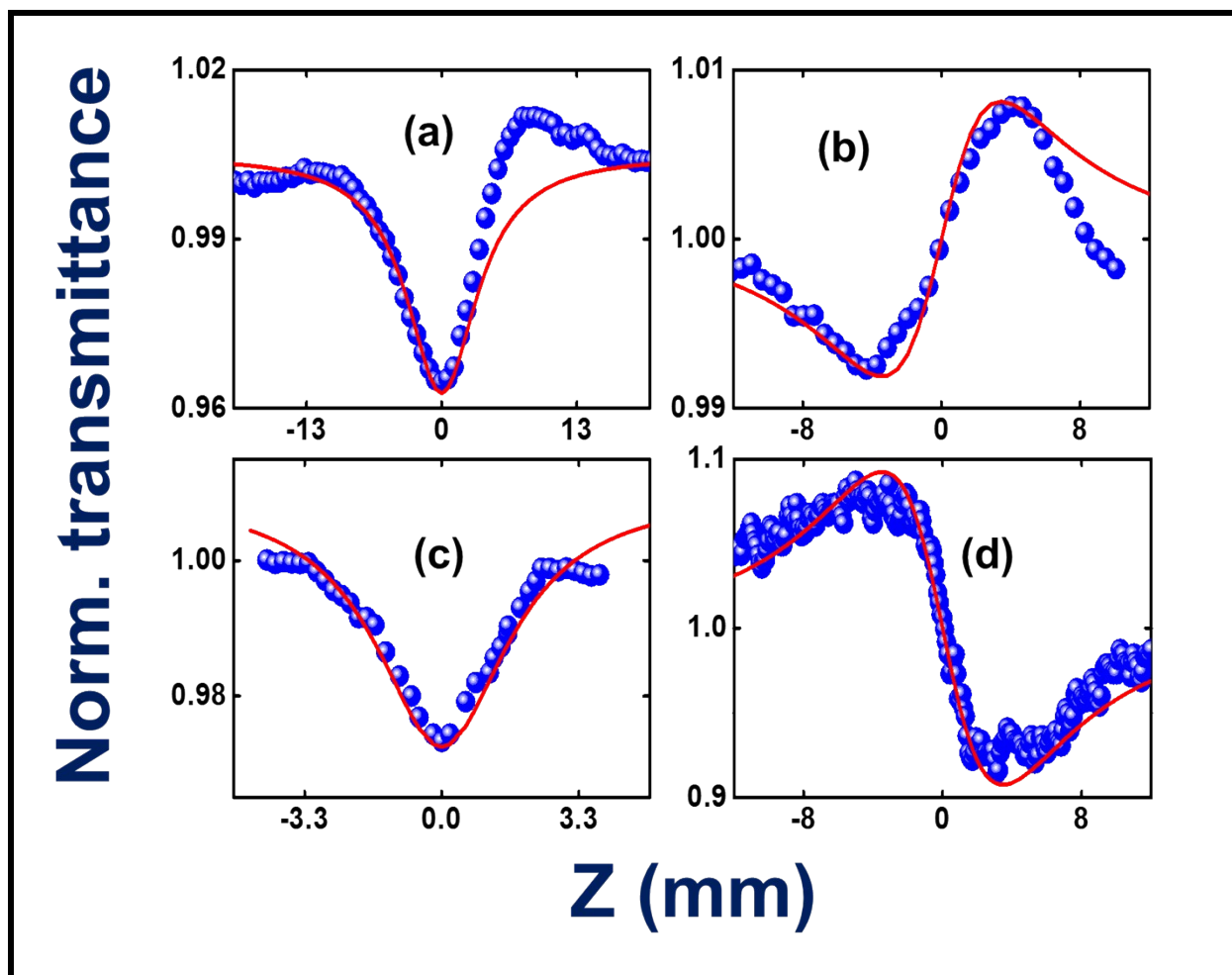


Fig. S22. Fluorescence spectra of TBC-CBZ in various solvents.



**Fig. S23.** *In-situ* UV-Vis spectro-electrochemical changes of TBC-CBZ. a)  $E_{app} = 0.90$  V b)  $E_{app} = 1.60$  V c)  $E_{app} = -1.30$  V.



**Fig. S24 .** NLO optical data (a) OA (b) CA of DCM solvent under excitation of femtosecond 1 kHz, 50 fs, 800 nm pulses. NLO optical data (c) OA (d) CA of DCM solvent under the excitation of femtosecond 80 MHz, 150 fs, 800 nm pulses. 3D blue spheres and red continuous lines correspondingly represent experimental data and theoretically fitted curves.



## References

1. J. V. S. Krishna, D. Koteswar, T. H. Chowdhury, S. P. Singh, I. Bedja, A. Islam, L. Giribabu, Efficient near IR porphyrins containing a triphenylamine-substituted anthryl donating group for dye sensitized solar cells. *J. Mater. Chem. C.*, 2019,**7**, 13594-13605. DOI: 10.1039/c9tc03943k
2. D. Becke, Density-functional thermochemistry. III. The role of exact exchange. *J. Chem. Phys.*, 1993, **98**, 5648. <https://doi.org/10.1063/1.464913>
3. G. A. Peterson, M. A. Al-Laham, A complete basis set model chemistry. II. Open-shell systems and the total energies of the first-row atoms. *J. Chem. Phys.*, 1991, **94**, 6081. <https://doi.org/10.1063/1.460447>
4. M. J. Frisch, G. W. Trucks, H. B. Schlegel, G. E. Scuseria, M. Robb, A. J. R. Cheeseman, V. G. Zakrzewski, J. A. Montgomery, R. E. Stratmann, J. C. Burant, S. Dapprich, J. M. Millam, A. D. Daniels, K. N. Kudin, M. C. Strain, O. Farkas, et al., Gaussian 09, Gaussian, Inc., Pittsburgh PA, 2009.
5. S. Miertus, E. Scrocco, J. Tomasi, Electrostatic interaction of a solute with a continuum. A direct utilizaion of AB initio molecular potentials for the prevision of solvent effects *J. Chem. Phys.*, 1981, **55**, 117. [https://doi.org/10.1016/0301-0104\(81\)85090-2](https://doi.org/10.1016/0301-0104(81)85090-2)
6. M. Cossi, V. Barone, R. Cammi, J. Tomasi, Ab initio study of solvated molecules: a new implementation of the polarizable continuum model. *Chem. Phys. Lett.*, 1996, **255**, 327. [https://doi.org/10.1016/0009-2614\(96\)00349-1](https://doi.org/10.1016/0009-2614(96)00349-1)
7. N. M. O'Boyle, A. L. Tenderholt, K. M. Langner, cclib: a library for package-independent computational chemistry algorithms. *J. Comput. Chem.*, 2008, **29**, 839. DOI: [10.1002/jcc.20823](https://doi.org/10.1002/jcc.20823)
8. R. Dennington, T. Keith, J. Millam, GaussView, version 5, Semichem Inc., Shawnee Mission KS, 2009.